RERTR 2009 — 31st INTERNATIONAL MEETING ON
REDUCED ENRICHMENT FOR RESEARCH AND TEST REACTORS

November 1-5, 2009
Kempinski Hotel Beijing Lufthansa Center
Beijing, China

IN-SITU HIGH TEMPERATURE NEUTRON DIFFRACTION STUDY OF PHASE EVOLUTION IN U-7wt% Mo/Al AND U-7wt% Mo/Al-5wt% SI FUEL RODS

Jae Ho Yang, Ho Jin Ryu and Jong Man Park
Innovative Nuclear Fuel Division
Korea Atomic Energy Research Institute,
1045 Daedeokdaero, Yuseong-gu, 305-353 Daejeon-Korea

ABSTRACT

In-situ phase evolutions of atomized U-7wt% Mo fuel particles dispersed in an Al or Al-5wt% Si matrix were investigated at 550°C by an out-of-pile neutron diffraction method. Homogeneous γ-UMo fuel particles were decomposed to a mixture of α-U and γ'-U_2Mo (or Mo-rich γ-UMo) phases in the early stage of annealing. The kinetics of phase decomposition in fuel particles was found to be independent on the matrix composition. The dominant interaction phase between the fuel particle and matrix was identified as the UAl_3 type cubic phase. The kinetics of interaction growth between the fuel particles and matrix was depends on the matrix composition. In-situ neutron diffraction patterns showed that a Si addition in the Al matrix retarded the formation and growth of the UAl_3 type interaction phase.

1. Introduction

Uranium-molybdenum alloy particle dispersion fuel in an aluminum matrix with a high uranium density has been developed for a high performance research reactor in the RERTR program under the non-proliferation policy [1]. Although the results of irradiation tests are promising, an unacceptable volume expansion caused by interaction layer and subsequent high porosity formation between the UMo fuel particles and Al matrix has been an obstacle for further development of this fuel.

Several relevant studies to understand the detailed inter-diffusion mechanism in the interaction layer (IL) and to mitigate its growth are under progress. Previous diffusion studies revealed that the dominant phases in interaction layer of (U,Mo)/Al system is $(U,Mo)Al_3$. Interaction phases of $(U,Mo)Al_4$ was also reported [2]. Resent studies have shown that the ternary phase of $UMo_{2-x}Al_{20+x}$ forms near the Al matrix while $U_6Mo_{4+x}Al_{43\mu-x}$ does near the UMo particle [3,4].

On the basis of previous works on U-Al alloy available in the literature, the group at Argonne National Laboratory proposed to modify the matrix by adding Si to suppress the formation of UAl_4 type interaction phase and thereby reduce the swelling of dispersion fuel under the irradiation [5]. Previous out-of-pile and in-pile tests show accumulation of Si in IL and IL

thickness reduction compared to the fuels between UMo and pure Al [6,7]. In a recent study [8] it was shown that Zr additions to U-Mo enhance the effect of Si in Al. It is believed that Si promotes the formation of a $U(AlSi)_3$ type phase that is more stable during irradiation. A recent synchrotron XRD study [9] has also shown that U_3Si_5 and $Al_{20}Mo_2U$ compounds also form in IL.

From the performance analysis point of view, it is necessary to identify the interaction phases in interaction layers. During irradiation, the ILs are amorphous at much lower temperatures (at the highest ~200 ^oC). Strictly speaking, therefore, no phases exist in the ILs [10]. The present study is meaningful to understand the underlying mechanism. It is also important to know the times when each phase first emerges. In U vs Al reactions, the post test results show that the dominant phase is UAl_3. Therefore, knowing the fractions of each phase as a function of time can be valuable information for extrapolation to irradiation behavior. Furthermore, not a single work was performed on characterization of reaction phases at in-situ reaction temperatures.

In this study, we perform in-situ tests of out-of-pile neutron diffractions of U-7wt% Mo fuel/Al and U-7wt% Mo fuel/Al-5wt% Si dispersion fuel rods to analyze the phase evolution during annealing at 550^oC. Phase decomposition behavior of γ-(U,Mo) was also investigated. The crystal structure of the dominant interaction phase was characterized and its volume fraction was measured as a function of time.

2. Experimental procedures

U–7wt%Mo alloy was melted by a vacuum induction method using a depleted uranium lump (99.9 wt%) and Mo (99.7 wt%) in a zirconia crucible, and then centrifugally atomized to U–7Mo alloy powders. U–Mo powders of 210–297 μm in diameter and pure Al powders or 5wt% Si added Al powders were mixed in a V-mixer with a rotation speed of 90 rpm for 1 h and hot-extruded at 400^oC with an extrusion ratio of 38:1. U–loading of dispersion fuel was 3.0 gU/cm^3. The dimensions of the sample fuel rods were 50mm in height and 6mm in diameter.

The in-situ neutron powder diffraction patterns of the sample dispersion fuel rods were collected during the high temperature annealing at 550^oC with a high-resolution powder diffractometer [λ = 1.8339 Å and $\sin(\theta_{max})/\lambda$ =0.527 Å^{-1}] at the HANARO reactor, Korea Atomic Energy Research Institute (KAERI). A fuel rod was equipped in a lab-made high temperature furnace. The sample was heated up to 550^oC with a constant heating rate of 5K/min. When the sample was reached at target temperature, the neutron diffraction was started. It took 20 minutes to obtain one set of diffraction pattern. A total of 30 diffraction patterns were obtained for each sample. Therefore total annealing time for an individual fuel rod was 10h. The neutron fluxes from the ST2 channel of the reactor were monochromated by a vertically focusing composite Ge monochromator at a 90^o take-off position.

The microstructure of U–Mo/Al dispersion fuels were characterized by scanning electron microscopy (SEM). The samples after neutron diffraction experiments were sectioned and polished. Concentration profiles of reaction layers were obtained by point-to-point counting techniques using a Phillips XL30 microprobe equipped with an energy dispersive spectrometer.

The Rietveld method and the full pattern analysis method were used to analyze the phase evolution during the annealing of dispersion fuel rods. Based on the results from EDS work for annealed sample and the collected structural data from the literature [10-14], we

developed a model to interpret the measured diffraction patterns. To verify the model, we apply the model to the 30th measured diffraction pattern by the Rietveld method. A quantitative analysis was made by a full pattern analysis method. The structural parameters which were obtained by the Rietveld method were set constant, and the relative proportion of various phase in fuel rods were calculated by fitting the scale factors of component phases. All of the neutron diffraction analysis was carried out by programs in FullProf-suite including the FULLPROF2000 program (RodrõÂguez-Carvajal, 2001).

3. Results and discussion

3.1. Microstructure analysis of the dispersion fuel rods after the neutron diffraction

3.1.1. U-7wt%Mo/Al fuel rod.

Microstructure of the ILs between the U-Mo fuel and the Al matrix after neutron diffraction tests at 550°C was examined by using SEM. Fig. 1(a) shows a BS image of the fuel cross section. The ILs are developed well. The shape and thickness of ILs of fuel particles are irregular and inhomogeneous. Measured thickness was ranged from a few μm to over 100μm. This non-uniformity of IL might be due to a decomposition of the gamma phase, an inhomogeneous contact pressure between the particles and matrix and the presence of a surface oxide on the matrix and fuel particles.

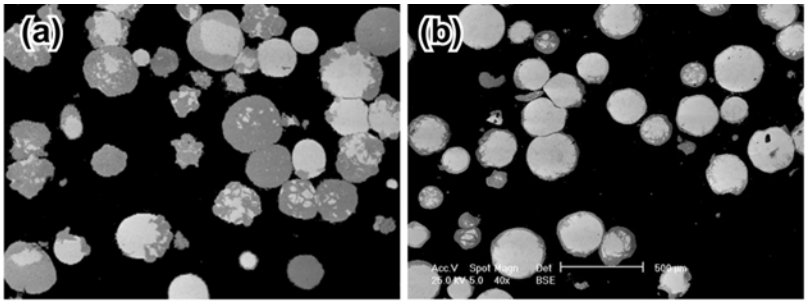

Fig. 1. Back scattered SEM images of dispersion fuel rods after the neutron diffraction test at 550°C for 10hrs. (a) U-7wt%Mo/Al, (b)U-7wt%Mo/Al-5wt%Si

Chemical composition variation along the ILs in the dispersion fuels was measured by EDS. We have selected several ILs having different thickness and shape for EDS investigation. Fig. 2 shows the typical examples of measured composition profiles along the ILs. In the Al side of the IL, we could observe thin and white island particles. An EDS profile (Fig. 2(c)) and a corresponding qualitative WDS profile (Fig. 2(d)) indicate that these white particles are an oxide phase of (U,Mo). The composition of ILs was measured to $(U,Mo)Al_3$. The Mo depleted from $(U,Mo)Al_3$ ILs was piled up in the fuel and IL boundary. The BS image of the un-reacted fuel particle clearly revealed that the γ-UMo phase was decomposed to a mixture of α-U and γ'-U_2Mo (or Mo-rich γ-UMo) phases during annealing.

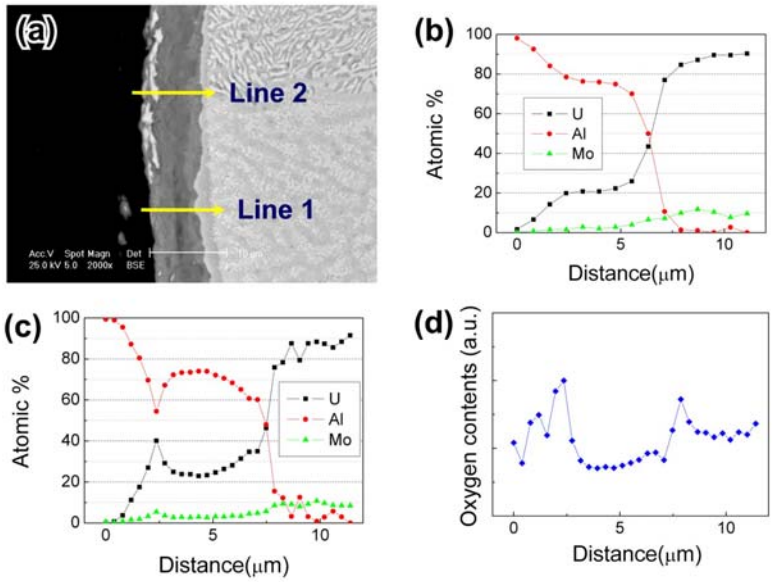

Fig. 2. The back scattered SEM photograph and the composition profile of U-7Mo/Al dispersion fuel along the interaction layers. (a) BS image, (b) composition profile along the line 1, (c) composition profile along the line 2, and (d) qualitative WDS profile for oxygen along the line 2

In order to verify the composition of the dominant phase in ILs, the measured composition data in the line profiles are plotted in a single ternary diagram shown in Fig.3. Most of composition data of ILs are located in the narrow composition range as denoted by circle in Fig.3. The atomic ratio Al/(U+Mo) is about 3, implying that the main interaction product is a (U,Mo)Al_3 type cubic phase. This result is basically similar to those from out-of-pile diffusion couple tests. However, the measured composition data are found almost in a single interaction line between Al and (U7wt%Mo) alloy. No case for a composition high in Mo was measured, indicating the absence of ternary compounds such as $U_6Mo_4Al_{43}$ or UMo_2Al_{20}.

3.1.2. U-7wt%Mo/Al-5wt%Si fuel rod.

Comparison of the BS image of U-7Mo/Al-5Si fuel (shown in Fig. 1(b)) with that of the U-7Mo/Al (shown in Fig. 1(a)) clearly shows that evolution of IL was suppressed effectively by the addition of Si. Fig. 4 shows a typical image of fuel particle and the composition mapping for Si. Si was diffused in IL and made a Si rich phase. However, the Si map shown in Fig. 4(b) indicates that the Si content is lower in the region with a thicker IL.
Fig. 5 and Fig. 6 show the Si mapping images and composition profiles along the IL obtained at the regions marked by R1 and R2 in Fig. 4(a), respectively. As shown in Fig. 5 (b), Si is accumulated in the IL. The ratio of (Al+Si)/(U+Mo) of IL is about 1.7 and this ratio is far less than 3 that is the ratio of Al/(U+Mo) of the dominant interaction phase in the (U,Mo)/Al system. However, the (Al+Si)/(U+Mo) ratio increases in the thick IL region (R2), in which the IL appeared to have two sub-layers with different compositions. The (Al+Si) to (U+Mo) ratio of outer IL (Al-side) is about 3 which corresponds to the composition of (U,Mo)Al_3 in the (U,Mo)/Al system. In fuel side of IL, a high Si content was found.

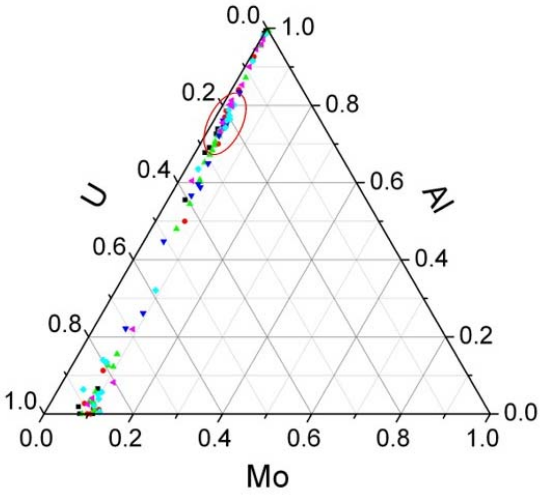

Fig. 3. Collection of point to point composition data of interaction layers for (U,Mo)/Al system.

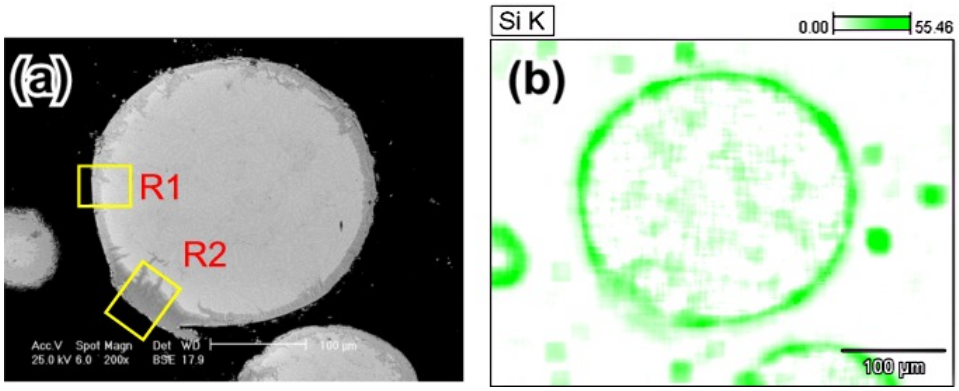

Fig. 4. (a) BS image of a fuel particle and (b) the Si mapping image

The whole data from point-to-point measurement along the several ILs were plotted in a pseudo ternary diagram (U+Mo)+Al+Si, Fig.7. Most of the measured data are confined in two distinct composition ranges due to their population and therefore can be categorized into two groups as marked by A and B in the figure. The (Al+Si) to (U+Mo) ratio of group A is ranged between 1 and 2. That of B is about 3. From line composition profile measurements, it was found that thin ILs consists of a single layer having same composition. The (Al+Si) to (U+Mo) ratio low and the Si content appear to be high in thin ILs. The thick ILs, however, appeared to have two sub-layers with different compositions. The Al contents increased and Si contents rather discretely decreased in thick layers. This result might imply that the (U,Mo) and Si composed the Si-rich phase (U,Mo)-Si compound at the early stage of annealing. As Al diffused further in the IL, Si content became diluted with Al, (Al+Si) to (U+Mo) ratio increased, finally the dominant phase of IL converted to $(U,Mo)(Al,Si)_3$ type phase. The tentative diffusion path of IL in (U,Mo)/(Al+Si) system was denoted in Fig.7.

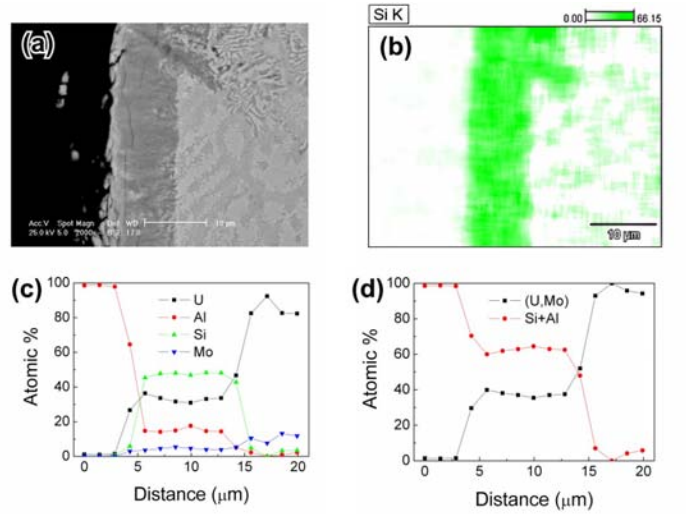

Fig. 5. The BS photograph and the composition profile along the interaction layer marked by R1 in Fig. 4. (a) BS image, (b) Si mapping image of IL, (c) composition profile for each elements along the IL, and (d) (U+Mo) vs. (SI+Al) plot.

3.2. Interaction phase characterization by in-situ neutron diffraction patterns.

3.2.1. U-7wt%Mo/Al fuel rod.

According to the EDS work given in 3.1.1., it is expected that there are five kinds of phase in the U-7wt%Mo/Al fuel rod. Raw fuel rod consists of homogeneous γ-UMo fuel particles and Al matrix. As the annealing time elapsed, γ-UMo particles in fuel rod were decomposed to a mixture of α-U and γ′-U_2Mo (or Mo-rich γ-UMo) and (U,Mo)Al_3 type interaction phase began to appear.

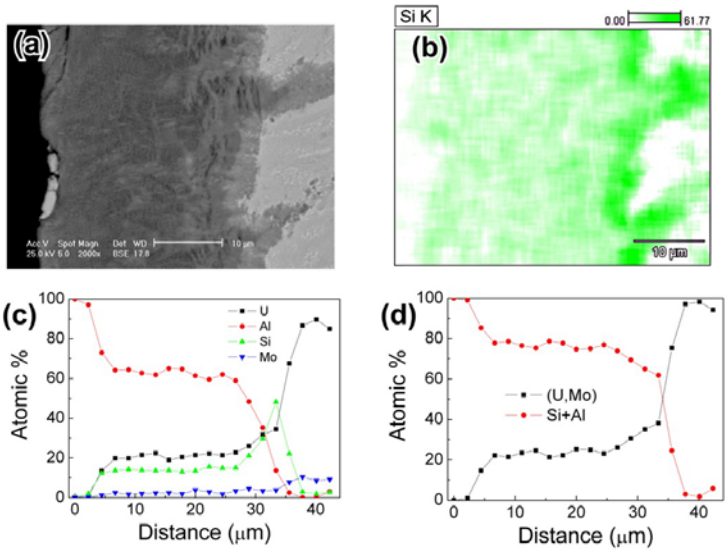

Fig. 6. The BS photograph and the composition profile along the interaction layer marked by R2 in Fig. 4. (a) BS image, (b) Si mapping image of IL, (c) composition profile for each elements along the IL, and (d) (U+Mo) vs. (SI+Al) plot.

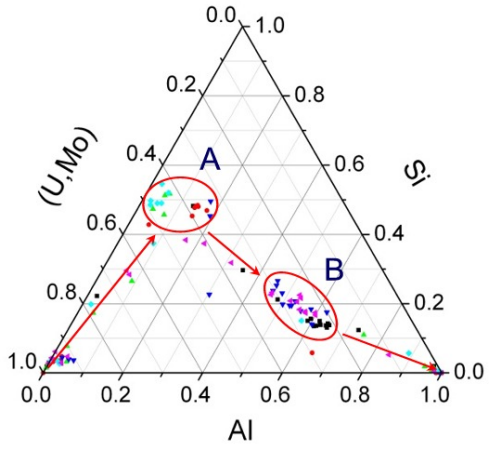

Fig. 7. Ternary diagram for whole point to point composition data of interaction layers for (U,Mo)/(AlSi) system.

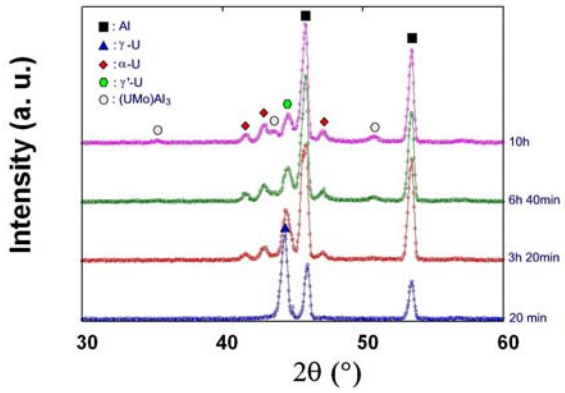

Fig. 8. Selected neutron diffraction patterns of (U,Mo)/Al system

Fig. 8 shows an example of neutron diffraction patterns. The annealed fuel rod, after the 30th diffraction test, consists of Al, α-U, γ-UMo, γ′-U_2Mo (or Mo-rich γ-UMo) and the interaction phase. The interaction phase is likely to be UAl3 type cubic phase according to the positions of the peaks. These phases observed in a neutron diffraction pattern are coincident with those predicted in the EDS work. The structural parameters of existing phases were obtained from literature, and the Rietveld analysis was conducted for a 30th pattern using collected parameters.

The calculated profile fits to the experimental neutron intensity data and the difference profile for the refinement are shown in Fig. 9. The calculated profile matches well with the measured data. There are some un-defined low intensity peaks in the measured profile. The information from these peaks is so week to conduct refinement. When we consider extra peak positions, those peaks seem to be related with UAl_4 type phase. Therefore, it is expected that small amount of crystalline (U,Mo)Al_4 phase exists in the fuel rod. It was reported that ternary compounds of UMo_2Al_{20} or $U_6Mo_7Al_{40}$ are also observed in IL. However, the diffraction peak from those compounds couldn't be found in this profile.

Based on the Rietveld result for the 30th neutron diffraction profile, we have conducted a quantitative analysis of remained diffraction profiles by full pattern analysis method. The fractions of existing phases in fuel rods were calculated by fitting the scale factors of component phases. Fig. 10 shows the percentage of integrated intensity of component phases to the total integrated intensity. It appears that γ-UMo fuel particles were

decomposed to a mixture of α-U and γ′-U_2Mo (or Mo-rich γ-UMo) phases in the early stage of annealing, which is consistent with the data by Van Thyne [16]. Whereas, the appearance of interaction phase of (UMo)Al_3 requires some incubation time. The α-U and γ′-U_2Mo (or Mo-rich γ-UMo) phases increased with time and the curves have with a parabolic shape. The (U,Mo)Al_3 interaction phase increased lineally with time.

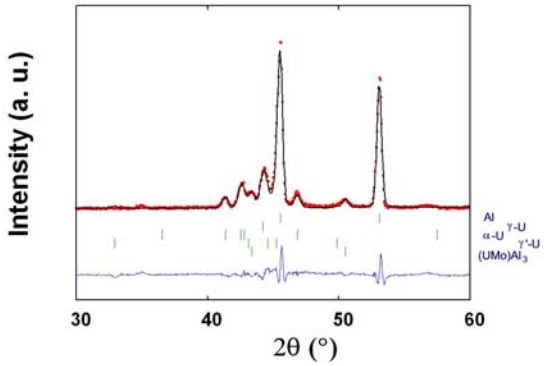

Fig. 9. 30th Neutron diffraction powder patterns of a (UMo)/Al fuel rod (circles: observed; line: calculated) with the difference profiles shown below.

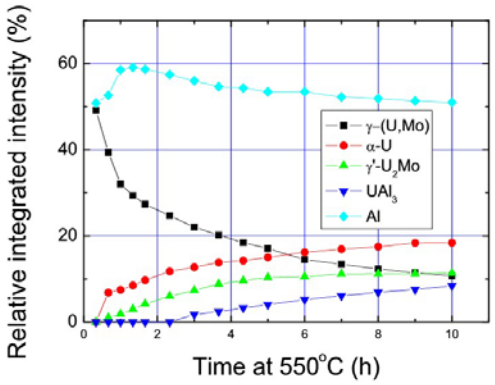

Fig. 10. The percentage of integrated intensity of component phases to the total integrated intensity in (UMo)/Al fuel rod.

3.2.2. U-7wt%Mo/Al-5wt% Si fuel rod.

Fig. 7 indicates that there are two distinct composition regions of interaction phase in U-7wt%Mo/Al-5wt% Si system. Similarly to the U-7wt%Mo/Al system, the (U,Mo)$(Al,Si)_3$ type cubic phase is the dominant interaction phase. In addition, Si-rich phase is also expected to exist. Previous out-of-pile diffusion investigations found a high Si content in the ILs and showed that five Si-rich phases in this ILs are possible to form depending on the condition. These phases include binary compounds such as USi_{2-x}, USi_2, U_3Si_5 and ternary compounds such as U_3Al_2 Si_3, U_3AlSi_3. Fig. 11. shows the selected neutron diffraction patterns. Diffraction peaks from Al, Si,α-U, γ-UMo and γ′-U_2Mo (or Mo-rich γ-UMo) found in the 30th neutron diffraction profile. When we compare 30th pattern with that in Fig. 8, the intensity of a diffraction peak (denoted by filled circle) from UAl_3 type interaction phase was largely depressed. This means that the development of IL was effectively reduced in this system.
The calculated profile fits to the experimental neutron intensity data and the difference profile for the refinement are shown in Fig. 12. The calculated profile matches relatively well with the measured data. Though the existence of binary or ternary compounds of Si-rich phase in IL was reported in literature, the diffraction peaks from those compounds could not

be found in this profile. Based on the Rietveld result for the 30th neutron diffraction profile, we have conducted a quantitative analysis of remained diffraction profiles by a full pattern analysis method. Fig. 13 shows the percentage of integrated intensity of the component phase to the total integrated intensity. Decomposition behavior of γ-UMo fuel particles with time is very similar to that in (U,Mo)/Al system. However, the appearance of interaction phase is much delayed in this system. In addition, the growth of interaction phase is suppressed in this system.

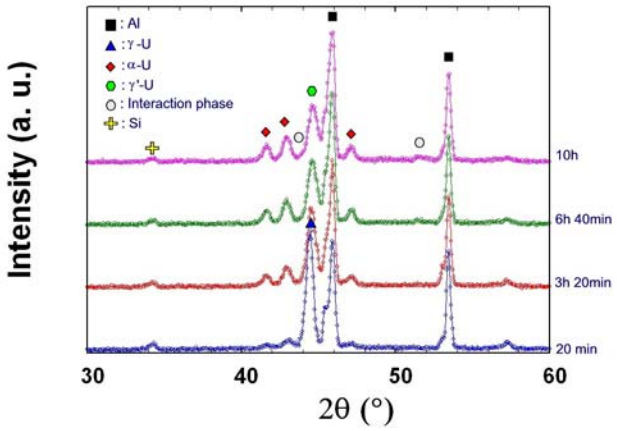

Fig. 11. Selected neutron diffraction patterns of (U,Mo)/(AlSi) system

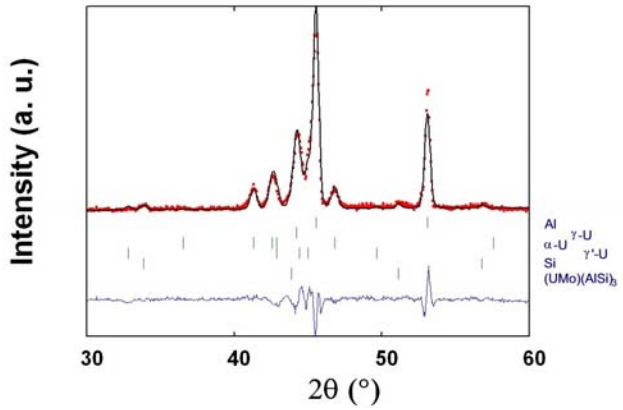

Fig. 12. 30th Neutron diffraction powder patterns of a (UMo)/(AlSi) fuel rod (circles: observed; line: calculated) with the difference profiles shown below.

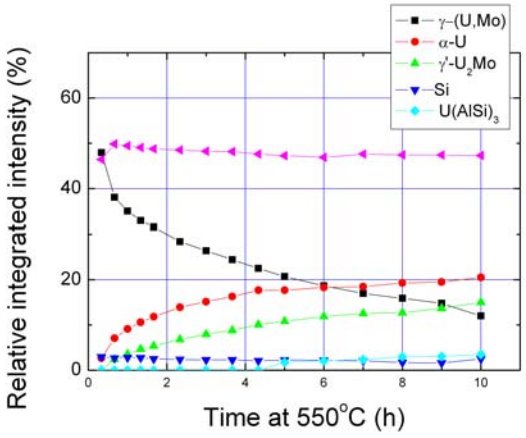

Fig. 13. The percentage of integrated intensity of component phases to the total integrated intensity in (UMo)/(AlSi) fuel rod.

4. Conclusions

In-situ phase evolutions in U-7wt% Mo/Al dispersion fuel rods and in U-7wt% Mo/Al-5wt% Si dispersion fuel rods were observed during out-of-pile annealing tests at 550°C by using neutron diffraction data. γ-UMo fuel particles were decomposed less than 30 min to a mixture of α-U and γ'-U_2Mo (or Mo-rich γ-UMo) phases regardless of the type of matrix.
The dominant interaction phase of both systems is identified as UAl_3 type cubic phase. Other binary or ternary interaction phases were not observed in this study. Quantitative analysis reveals that the existence of Si in the Al matrix effectively prevents the formation of phases having a high Al/(U+Mo) ratio and suppresses the growth of UAl_3 type interaction phase.

4. References

[1] J.L. Snelgrove, G.L. Hofman, M.K. Meyer, C.L. Trybus, T.C. Wiencek, Nuclear Engineering and Design 178 (1997) 119–126.
[2] H.J. Ryu, Y.S. Han, J.M. Park, S.D. Park, C.K. Kim, J. Nucl. Mater. 321 (2003) 210.
[3] F. Mazaudier, C. Proye, F. Hodaj, J. Nucl. Mater. 377 (2008) 476.
[4] H. Noel, O. Tougait, S. Dubois, J. Nucl. Mater. 389 (2009) 93.
[5] Y.S. Kim, G.L. Hofman, H.J. Ryu, J. Rest, in: Proceedings of the 2005 RERTR International Meeting, Boston, USA, November 6–10, 2005.
[6] M. Mirandou, S. Arico, L. Gribaudo, S. Balart, in: Proceedings of the 2005 RERTR International Meeting, Boston, USA, November 6–10, 2005.
[7] Y.S. Kim, G.L. Hofman, H.J. Ryu, M.R. Finlay, D. Wachs, in: Proceedings of the 2006 RERTR International Meeting, Cape Town, South Africa, October 29–November 2, 2006.
[8] J.M. Park, H.J. Ryu, S.J. Oh, D.B. Lee, C.K. Kim, Y.S. Kim, G.L. Hofman, J. Nucl. Mater. 374 (2008) 422.
[9] M. Mirandou, S. Arico, M. Rosenbursch, M. Ortiz, S. Balart, L. Gribaudo, J. Nucl. Mater. 384 (2009) 268.
[10] H.J. Ryu, Y.S. Kim, G.I. Hofman, J. Nucl. Mater. 385 (2009) 623.
[11] P. Rogl, H. Noel, Aluminium-Silicon-Uranium, in *Ternary Alloy Systems, Subvolume C Non-ferrous metal system, Part4. Selected Nuclear Materials and Engineering Systems*, Edited by G. Effenberg and S. Ilyenko, Springer, 2007.
[12] T. Le Bihan, S. Heathman, M. Idiri, G. H. Lander, J. M. Wills, A. C. Lawson, and A. Lindbaum, Physical Review B 67 (2003) 134102
[13] V.Y. Zenou, G. Kimmel, C. Cotler, M. Aizenshtein, Journal of Alloys and Compounds 329 (2001) 189.
[14] E.K. Halteman, Acta Cryst. 10 (1957) 166
[15] F. Weitzer, M. Potel, H. Noel, P. Rogl, Journal of Solid State Chemistry 111 (1994) 267.
[16] R.J. Van Thyne, Uranium Alloys Newsletter, 13, Nov. 1955.

Acknowledgments

This study was supported by National Nuclear R&D Program by Ministry of Education, Science and Technology of Republic of Korea. The authors wish to acknowledge Dr. Y.N. Choi and K.Y. Kim for their contributions in neutron diffraction experiment. The authors also wish to acknowledge H.M. Kwon of PIEF at KAERI for their assistance in SEM and EDS study. Thanks are also due to Dr. Y.S Kim at ANL for helpful comments.